Multi-Objective Optimization of Process Parameters for Drilling Fiber-Metal Laminate Using a Hybrid GRA-PCA Approach

Ergün Ekici
Associate Professor
Çanakkale Onsekiz Mart University
Faculty of Engineering
Turkey

Ali Riza Motorcu
Professor
Çanakkale Onsekiz Mart University
Faculty of Engineering
Turkey

Gültekin Uzun
Associate Professor
Gazi University
Faculty of Technology
Turkey

This study investigated the effects of drilling parameters and cutting tool coating conditions on the thrust force, surface roughness, and delamination factor in the drilling of fiber-reinforced carbon reinforced aluminum laminate (CARALL) composite, a commercial type of fiber-metal laminate. Gray relational analysis (GRA) was used as a multi-objective optimization method to determine optimum processing parameters and principal component analysis (PCA) was used to determine the weights. According to the findings of this experimental study, the most effective control factors for the thrust force, surface roughnes, and delamination factor were the feed rate, tool coating condition-cutting speed interaction, and tool coating condition, with 93.87%, 66.504%, and 29.137% contribution rates, respectively. From the results of the GRA-PCA analysis, the optimum levels of the control factors were determined as 110 m/min cutting speed, 0.1 mm/rev feed rate, and the uncoated tool.

Keywords: *Fiber-metal laminate, CARALL composite, drilling, thrust force, surface roughness, delamination.*

1. INTRODUCTION

In recent years, research interest in the field of engineering applications has increasingly shifted from traditional material to composite material (CM) applications in various engineering industries [1, 2]. Fiber-metal laminate (FML) is a composite material system consisting of varying layers of thin metal sheets and composite prepregs. These FMLs have seen wide application for structural components in the aerospace and defense industries due to their unique properties that combine fatigue and impact resistance with relatively low density, flame (high burning) and corrosion resistance [3-5]. The most common commercialized FMLs are aramid reinforced aluminum laminate (ARALL), high-strength glass-fiber-based glass reinforced aluminum laminate (GLARE), and carbon-based carbon reinforced aluminum laminate (CARALL) composites [6].

In CARALL, which was developed against ARALL's low compression resistance, carbon fibers are laid between aluminum plates. Because of these features of CARALL, aircraft parts can be produced that have the same strength but are lighter than metals [7]. The assembly of aircraft structural parts is performed using fasteners and riveted bolts that require drilling a large number of holes. The number of holes required can range from 300,000 holes in a jet fighter to 1.5-3 million holes in a commercial aircraft [8]. Throughout their service life, FRP composites lose strength due to delamination [9]. The unique properties of fiber-reinforced polymers, such as tough and abrasive carbon fibers and a heat-sensitive matrix, make drilling more difficult and expensive [10]. Although it is sufficient to use appropriate cutting parameters to improve the surface quality of the holes in fiber-reinforced composites, CARALL laminates require different cutting parameters due to their mixed structure of aluminum and carbon fiber.

The importance of research on the drilling of FMLs is increasingly revealed in the literature. Pawar et al. focused on the relative influence of cutting parameters and tool geometry on delamination, burr formation, and cutting mechanics during the drilling of GLARE. They investigated thrust force, torque, and acoustic emission (AE) signals to analyze the cutting mechanism and the formation of burr and delamination [11]. Tyczynski et al. analyzed the machinability of carbon fiber reinforced polymer (CFRP), glass fiber reinforced polymer (GFRP), and GLARE-type composites (geometric properties, volume ratios, and mechanical properties of the components of each composite) in the drilling process [12]. Coesel recommended the use of coated tools instead of high-speed steel and uncoated carbide tools because they provided high wear resistance and hole quality against the abrasive structure of the fibers [13]. Giasin et al. reported that when drilling FMLs under dry cutting conditions, TiN-coated drills would yield the best results in terms of minimum roughness and burr formation. Moreover, TiN coatings performed better than TiAlN and AlTiN/TiAlN coatings when used only for short hole-drilling series, because of rapid tool degradation [14].

Giasin et al. modeled cutting forces using finite element analysis (FEA) and investigated the hole quality experimentally in the drilling of FEMs. The experimental results indicated that the thrust force and torque

Received: January 2021, Accepted: February 2021
Correspondence to: Prof. Dr Ali Riza Motorcu
Faculty of Engineering, ÇOMÜ
Terzioğlu Campus, 17100, Çanakkale, Turkey
E-mail: armotorcu@comu.edu.tr
doi: 10.5937/fme2102356E

increased with increasing feed rate and decreased with increasing spindle speeds. The surface roughness varied between 1.5 and 2 μm, increasing with the increase in the feed rate and spindle speeds [15]. In another study, Giasin et al. conducted experimental research on the drilling of uni-directional GLARE FMLs. As a result of their study, it was observed that fiber orientation had no effect on cutting forces, whereas both feed rate and cutting speed had significant effects on cutting forces and hole quality [16].

In the present study, the effects of the coating type, cutting speed, and feed rate on the thrust force, surface roughness, and delamination factor were investigated using all experimental data and multi-objective optimization methods. Probability tests were carried out in accordance with the optimization of the experimental results. Principal component analysis (PCA) was applied together with the Taguchi-based multi-objective optimization technique of gray relational analysis (GRA) to investigate the drilling behavior of CARALL composites. This study is seen as a pioneer among new scientific studies because it examines the effects of cutting parameters on the problems of delamination, low surface quality, and high thrust force, all of which play an important role in the rejection of FML composites.

2. EXPERIMENTAL PROCEDURE

Information on the manufacturing of the composite materials, machinability tests, experimental design, and optimization methods, which constitute the content of this study, are presented under the following sub-headings, respectively.

2.1 Material and Methods

The CARALL material is comprised of metal (Al5754 alloy) and CFRP composite layers, respectively. Each CFRP plate consists of three layers of 245 g/m^2 woven carbon prepreg carbon fiber. In order to improve the carbon fiber-Al interface properties, the Al 5754 alloy was mechanically abraded with 400 mesh sandpaper, and the surfaces were then rinsed with pure water.

Before anodizing, the samples were etched with alkali for 6 min in 100 g/L NaOH eloctrolyte at 60 °C and rinsed with distilled water. The sample was then kept in 200 mL/L HNO_3 for 4 min at room temperature and rinsed with distilled water. Anodizing was carried out within 15 min in 180 g/L sulfuric acid electrolyte. After this application, the Al plates were placed in vacuum bags and CARALL production was started shortly thereafter (in less than 60 min).

The CARALL samples were prepared in a total of seven layers, including four carbon fiber layers and three Al layers, in 500 × 500 mm dimensions, as shown in Figure 1, and cured for 1 h at 125 °C under a press load of 15 tons.

After the CARALL material was produced, in order to conduct the drilling tests, experimental workpieces of 110 × 80 mm were cut using a water jet. Drilling experiments were carried out in a Johnford VMC 850 vertical machining center under dry cutting conditions. Uncoated and signum-coated carbide drills of 66 mm in total length and 6 mm in diameter with 118° tip and 30° helix angles were used in the experiments. Technical properties of the signum-coated carbide drills are presented in Table 1.

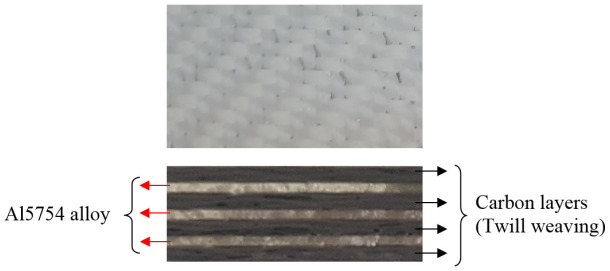

Figure 1. Top and side view of the CARALL sample.

2.2 Machinability Experiments

After the CARALL material was produced, the experimental workpieces of 110 × 80 mm were cut using a water jet in order to conduct the drilling tests. Drilling experiments were carried out in a Johnford VMC 850 vertical machining center under dry cutting conditions.

Table 1. Signum coating properties

Coating process	Physical Vapor Deposition
Layer structure	Multi-Layer Nano Composite
Thickness [μm]	3.0-5.0
Hardness [HV 5 g]	5500
Coating	TiAl/TiAlSiMoCr
Friction coefficient	0.5
Maximum operating temperature [°C]	800

A Kistler 9272 dynamometer was used for thrust force measurement and measurement results were determined using Dynoware software. The Mitutoyo Surftest-311 surface roughness measuring instrument was used to determine surface roughness. In the drilling of CFRP laminates, if the thrust force generated by the cutting tool exceeds the interlayer shear strength, it can cause two adjacent fabric layers to rupture at any point within the layer thickness. This situation, called "push-out", becomes more critical in the exit area, where the thickness of the uncut layer decreases and the CFRP has less resistance against the drilling thrust force. It has been reported in the literature that the delamination damage occurring at the hole exit is much higher compared to that at the hole input and that it has a more serious effect on the mechanical performance of the parts [17-20]. Therefore, hole exit delamination damage was investigated in this study. The extent of this type of damage is often measured by calculating the delamination factor (*Df*) [21-23]. Digital image processing is a convenient and widely used technique for analyzing geometric damage in CFRP. After the drilling experiments, hole exit delamination measurements were carried out using a Dino-Lite optical microscope. In damage measurements, the delamination factor was determined as the ratio of the maximum damage diameter (*Dmax*) to the drilled hole diameter (*D*) based on the conventional delamination dimension measurement. Dinocapture software was used to measure the delamination factor formed in the drilling of the CFRP.

2.3 Optimization Method

Taguchi experimental design (DoE) is a statistical technique used to examine many factors simultaneously and in the most economical way [24]. However, the Taguchi method is designed to optimize a single performance characteristic [25], whereas in most practical engineering problems, parameters cannot be set for one response alone because the goal will be to minimize and maximize some of the responses. Gray relational analysis (GRA) is used to determine the optimum levels of many input parameters in order to obtain the specified quality characteristics. To achieve this goal, the GRA uses the averages of multiple normalized targets to calculate the gray relational degree (GRD). However, the ambiguity and complexity of decisions regarding weight assignment must be eliminated. The accuracy of optimization can be improved by considering the weighting values of each response rather than the averages [26]. For this reason, principal component analysis (PCA), which is one of the effective methods for evaluating the weight values of the responses, is used to give weight to the GRDs in the output response. In this study, a Taguchi-based GRA-PCA hybrid method was used for the optimization of drilling parameters and cutting tool coating conditions in the drilling of the CARALL composite. The steps of this method are presented below.

2.4 Optimization Method

The Taguchi L_{18} orthogonal array was used as the experimental design for the three selected control factors. These control factors and their levels are given in Table 2.

Table 2. Taguchi L_{18} control factors and levels

Code	Control Factor	Levels		
		1	2	3
A	Tool Coating status, *T*	Uncoated (*T1*)	Signum-Coated (*T2*)	-
B	Cutting speed, *Vc* (m/min)	65	85	110
C	Feed rate, *f* (mm/rev)	0.1	0.14	0.2

In the Taguchi method, the experimental results obtained are converted to the S/N ratio (dbA). The S (signal) represents the desired value, and the N (noise) represents the undesired value [27]. Since, in an ideal situation, the thrust force, surface roughness, and hole exit delamination factor should be at the lowest levels the S/N ratios were calculated using Equation (1) by taking the criterion of "the smaller is better" as the reference. The % contributions of the control factors on the response variables were obtained by analysis of variance (ANOVA).

$$S/N = -10\log\left(\frac{1}{n}\sum_{i=1}^{n} yi^2\right) \tag{1}$$

In Equation (1), "S/N" is the S/N ratio, "*n*" is the number of observations, and "*y*" is the observed data.

2.5 Multi-Objective Optimization via GRA-PCA Hybrid Approach

The purpose of the GRA is to reduce multiple responses to a single response by normalizing the values of the recorded responses to range from 0 to 1. For the experimental data, the following steps were performed respectively:

Step 1. Data normalization

Since the data of the response variables come from different sources and the units are different from each other, the experimental data of each response is normalized by ranking them between 0 and 1. Normalization to the "the smaller is better" criterion was performed using Equation (2).

$$X_i^n(k) = \frac{\max X_i^0(k) - X_i^0(k)}{\max X_i^0(k) - \min X_i^0(k)} \tag{2}$$

where $X_i^n(k)$ is the normalized value, $X_i^0(k)$ is the original data, $\min X_i^0(k)$ and $\max X_i^0(k)$ are the minimum and maximum values of $X_i^0(k)$, respectively; "*i*" represents the number of observations and "*k*" represents the number of response variables.

Step 2. Calculation of the Gray Relational Coefficient (GRC)

The gray relational coefficient (GRC) expresses the relationship between ideal and actual experimental results, with ξ denoting the distinguishing coefficient that is defined in the range of 0 to 1, which is usually taken as 0.5 [28]. The GRC ($\xi i(k)$) can be calculated as:

$$\xi i(k) = \frac{\Delta_{\min} + \xi\Delta_{\max}}{\Delta_{0i}(k) + \xi\Delta_{\max}} \tag{3}$$

$$\Delta_{0i}(k) = \left|x_0(k) - x_i(k)\right| \tag{4}$$

$$\Delta_{\min} = \min_{i,k}\left|x_0(k) - x_i(k)\right| \tag{5}$$

$$\Delta_{\max} = \max_{i,k}\left|x_0(k) - x_i(k)\right| \tag{6}$$

Step 3. Calculation of weights

Principal component analysis (PCA) is one of the basic statistical approaches in which the dimensionality of a dataset is reduced by preserving the existing variations in the dataset and transforming the responses into a new dataset called the "principal component" [26]. The PCA approach was used to determine the response weights for the GRA. The correlation matrix, as the first step of the PCA, is calculated using Equation (7):

$$R_{jl} = \left[\frac{\operatorname{cov}\left(x_i(j), x_i(l)\right)}{\sigma x_i(j) \times \sigma x_i(l)}\right] \quad j = 1,2,...m; l = 1,2,...n \tag{7}$$

where $j = 1,2\ldots\ldots n$ and $l = 1,2\ldots\ldots n$; $cov(x_i(j), x_i(l))$ is the covariance of the $x_i(j)$ and $x_i(l)$ arrays, $\sigma x_i(j)$ is the standard deviation of the $x_i(j)$ array, and $\sigma x_i(l)$ is the standard deviation of the $x_i(l)$ array. Eigenvectors and their eigenvalues are obtained from the correlation coefficient matrix presented in Equation (8).

$$\left(R - \lambda_k I_m\right) \cdot V_{ilk} = 0 \tag{8}$$

In Equation (8), $k = 1, 2, ..., n$, and $V_{ilk} = [a_{k1}, a_{k2}, \ldots \ldots a_{kn}]$ represents the T eigenvectors corresponding to the eigenvalue λ_k.

The principal components are calculated using Equation (9):

$$y_{mk} = \sum_i^n X_m(i) * V_{ilk} \tag{9}$$

After the PCA, the eigenvalue of each principal component (the first is y_{m1}, the second is y_{m2}, etc.) is determined.

Step 4. Calculation of the Gray Relational Degree (GRD)

After calculating the weight, the final step of the GRA-PCA is utilized to determine the GRD. Equation (10) is used to calculate the GRD:

$$\alpha = \frac{1}{n} \sum_{k=1}^{n} \xi_k \times y_{mk} \tag{10}$$

In this study, the weight values of y_{mk} were obtained via PCA. The highest value of the GRD suggests the best possible parameters.

3. RESULTS AND DISCUSSION

Machinability analyses of the CARALL composites were performed in terms of drilling properties such as the thrust force, surface roughness, and hole exit delamination factor. The main effects of the control factors were evaluated using the Taguchi method. Parametric evaluation was carried out by applying the hybrid GRA-PCA technique with different mathematical models. The ANOVA was used to determine the factor-factor interactions that affected processing performances. The suitability of the data for optimization was carried out via the Anderson-Darling (AD) test.

3.1 Probability Tests

In the first stage of the analysis, the AD test was applied to reveal the suitability for normal distribution of the experimental results obtained according to the drilling parameters and coating condition. The probability plots are presented in Figure 2. When visibly examined, the probability test plots drawn at 95% confidence interval (CI) for the thrust force, surface roughness and delamination factor reveal that the data points do not exceed the 95% confidence limit and are approximately aligned with the midline. The P values calculated as 0.130, 0.434, and 0.414 for the thrust force, surface roughness and delamination factor, respectively, were greater than 0.05 and the AD values calculated for all three response variables (0.554, 0.349, and 0.358, respectively) were lower than the critical value of 0.752, as shown in these plots. These results support the normal distribution of the data and indicate that they can be used for optimization.

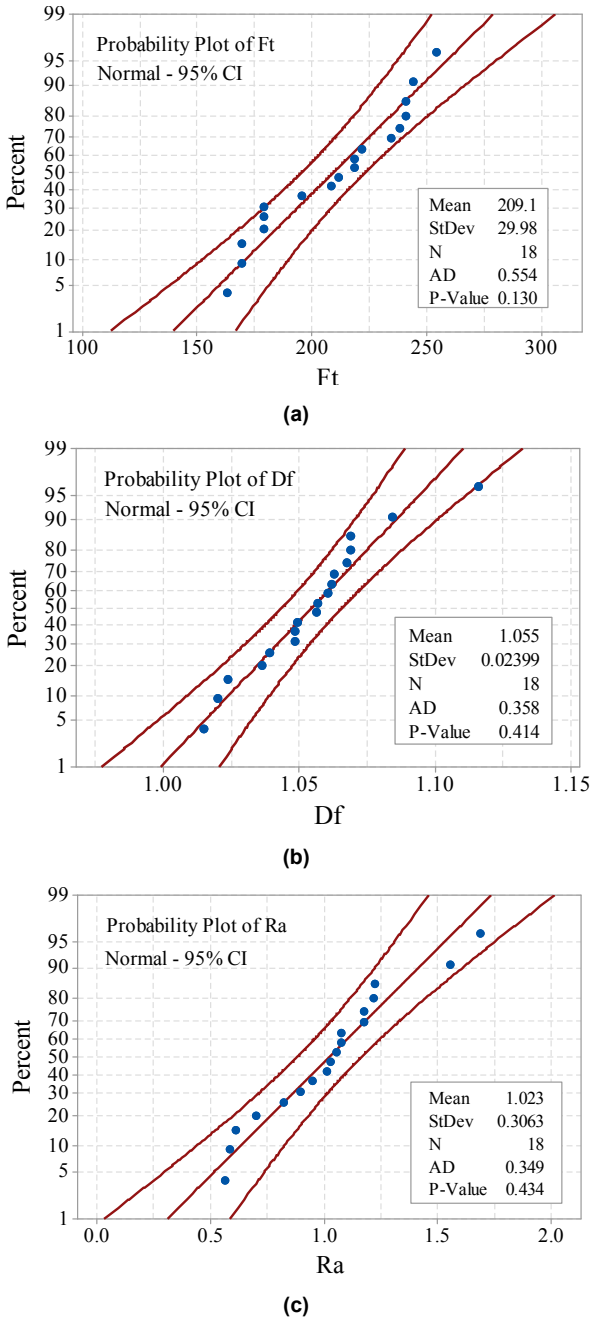

Figure 2. Probability plots: (a) thrust force, (b) average surface roughness, (c) delamination factor.

3.2 S/N Ratios and Analysis of Variance (ANOVA) to Determine the Effect of Processing Parameters on Performance Characteristics

The S/N ratio average plots were drawn in order to examine the main effects of the control factors (design parameters) affecting the thrust force, surface roughness, and delamination factor after the CARALL drilling process, depending on the control factors and tool coating condition. In addition, ANOVA was applied to investigate the % contribution ratio of the control factors, and the variance ratio values and % effects of each

control factor were calculated. The results of the drilling tests prepared in accordance with the L_{18} array and the S/N ratios (dBA) calculated according to the "the smaller is better" approach are presented in Table 3.

Table 3. Experimental results and their S/N ratios according to the Taguchi L_{18} orthogonal array

Trial No	Control factors			Experimental results			S/N ratios (dBA)		
	T	*Vc* [m/min]	*f* [mm/rev]	*Ft* (N)	*Ra* (μm)	*Df*	*Ft*	*Ra*	*Df*
1	Uncoated tool	65	0.1	179.040	1.074	1.015	-45.059	-0.620	-0.130
2		65	0.14	208.337	1.223	1.057	-46.375	-1.750	-0.480
3		65	0.2	240.883	1.686	1.067	-47.636	-4.538	-0.566
4		85	0.1	169.273	1.178	1.063	-44.572	-1.419	-0.531
5		85	0.14	221.350	0.950	1.048	-46.902	0.450	-0.409
6		85	0.2	238.227	0.898	1.048	-47.540	0.934	-0.411
7		110	0.1	162.763	0.586	1.020	-44.231	4.642	-0.172
8		110	0.14	195.313	0.611	1.036	-45.815	4.276	-0.310
9		110	0.2	234.373	0.564	1.024	-47.398	4.978	-0.206
10	Signum-coated tool	65	0.1	179.037	0.702	1.069	-45.059	3.076	-0.580
11		65	0.14	218.097	0.821	1.060	-46.773	1.716	-0.509
12		65	0.2	244.140	1.013	1.116	-47.753	-0.110	-0.954
13		85	0.1	169.273	1.027	1.069	-44.572	-0.231	-0.579
14		85	0.14	218.097	1.054	1.056	-46.773	-0.459	-0.474
15		85	0.2	240.883	1.220	1.084	-47.636	-1.725	-0.702
16		110	0.1	179.037	1.078	1.039	-45.059	-0.652	-0.332
17		110	0.14	211.587	1.176	1.062	-46.510	-1.410	-0.522
18		110	0.2	253.907	1.558	1.049	-48.093	-3.849	-0.418

3.2.1 Thrust force

The main effects plot for S/N ratios of thrust force (*Ft*) after drilling of the CARALL composite is presented in Figure 3. The drill chisel edge starts the drilling process by drilling the upper CFRP layer, then the Al and CFRP layers are drilled, respectively, and finally the drilling process is completed with the CFRP layer. Thrust forces are constantly changing during the drilling of this cascaded structure, and the thrust force generated when drilling the aluminum is much higher than when drilling the CFRP layer. The chip formation process in the Al5754 drilling is in the form of thermal softening and plastic deformation. In the CFRP layer, this process is in the form of separation of bonds and the formation of carbon fiber dust, as well as fiber breakage and matrix cracking.

Figure 2 shows that the uncoated tool performed better than the signum-coated tool in terms of tool thrust forces (according to the S/N ratio and "the smaller is better" approach). Xu et al. stated that uncoated drills performed better than TiAlN-coated tools by providing lower thrust force when drilling CFRP/Ti6Al4V stacks, and attributed this to the shorter length of the uncoated drill chisel edge [29]. Montoya et al. reported that when drilling CFRP/aluminum stacks, the uncoated tools resulted in lower cutting forces because of cutting edge sharpness compared to the coated tools [30]. Similarly, Ashrafi et al. stated that the uncoated tool produced lower thrust force than the coated tool when drilling CFRP/Al metallic stacks due to the fact that the uncoated tool had sharper cutting edges compared to the rounded edges of the coated tool. With the rounded cutting edge, the tool-workpiece contact area was greater in the feed direction, resulting in higher thrust force [31].

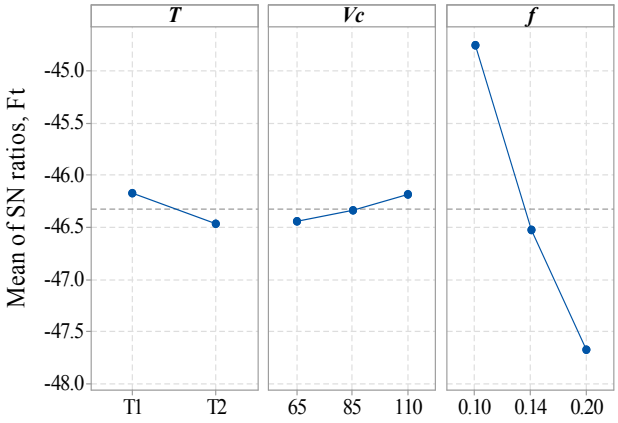

Figure 3. Main effects plot for S/N ratios of thrust force.

Thrust forces decreased steadily with increasing cutting speed. Increasing cutting speed increased the temperatures in the cutting zone and facilitated the plastic deformation of the aluminum plates, causing decreased thrust forces because of the softened epoxy. It appears that the increasing feed rate caused a serious increase in the thrust force. This situation was explained by the amount of chip removed per unit time. Similarly, many researchers have reported the serious physical and statistical effect of the feed rate during the drilling of CFRP [32-34]. Park et al. noted that the cutting edge of the cutting tool was exposed to more abrasive fibers and the cutting tool was exposed to more hole surface friction with an increasing feed rate [35]. The ANOVA was performed to determine the effects of the factors on processing performances [36]. Table 4 presents the ANOVA results for *Ft* depending on the control factors. The table shows that the tool coating status (*T*) and the feed rate (*f*) had a significant effect ($P < 0.05$) in terms of the main effects of the control factors, whereas *T*Vc* and *Vc*f* were significant in terms of factor interactions. The feed rate was seen as the most effective processing parameter with a 93.87% contribution ratio (Fig. 3). No significant effect (<2%) was found for tool coating status or cutting speed.

Table 4. ANOVA results for thrust force

Control factors	DoF	SS	MS	F_table	P	Contribution %
T	1	0.405	0.405	27.54	0.006*	1.467
Vc	2	0.2014	0.1007	6.85	0.051	0.730
f	2	25.9134	12.9567	880.99	0.00*	93.879
*T*Vc*	2	0.4593	0.2296	15.61	0.013*	1.664
*T*f*	2	0.0016	0.0008	0.05	0.949	0.006
*Vc*f*	4	0.5637	0.1409	9.58	0.025*	2.042
Residual Error (e)	4	0.0588	0.0147			0.213
Total	17	27.6031				100
R^2=99.8% Adjusted R^2=99.1%						
DoF: Degree of freedom, SS: Sum of squares, MS: Mean square *: Statistically significant effective parameter						

3.2.2 Surface roughness

Surface roughness (*Ra*) is affected by drilling parameters and tool geometry because of the continuous vibration of the cutting tool. Although gaps caused by fiber stripping, matrix degradation, and fiber matrix decomposition are common in CFRP layers in the drilling of FML, surface scratches occur in the Al layers due to the friction of the aluminum chips on the inner surface of the hole. Much higher *Ra* values occur in CFRP structures compared to Al alloys [31]. This is attributed to the heterogeneous nature of CFRP composites, the effect of fiber orientation on cutting, the brittle nature of the fibers, and fiber breakage during drilling [37]. In the drilling of the CARALL composite, CFRP was the main component that determined the *Ra* values. The main effects plot for S/N ratios of surface roughness in the drilling of the CARALL composite is presented in Figure 4. Lower *Ra* values were obtained with the uncoated tool compared to the signum-coated tool. The *Ra* values decreased with increasing cutting speed. Smearing of the molten epoxy resin was the primary mode of damage observed on the surface of the CFRP layer [38]. Perez et al. reported that increasing cutting speed reduced the temperature [39]. With increasing cutting speed, *Ra* values increased by decreasing the melting of the CFRP resin. Increasing feed rate also increased the *Ra* values. Ashrafi et al. stated that *Ra* values increased with the increasing feed rate in the drilling of CFRP/Al stacks [31]. Zitoune et al. found that when drilling CFRP/Al stacks at low feed rates (<0.1 mm/rev), the quality of the machined surface was better for all drills used. They attributed this to the fact that the 0.1 mm/rev feed rate facilitated the formation of discontinuous aluminum chips and stated that the measured roughness values (<3 μm) were lower [40]. The thickness measurements of the aluminum layers (0.5 mm) and the CFRP layers (≈0.75) in the CARALL composite sample were much lower compared to the metallic stacks.

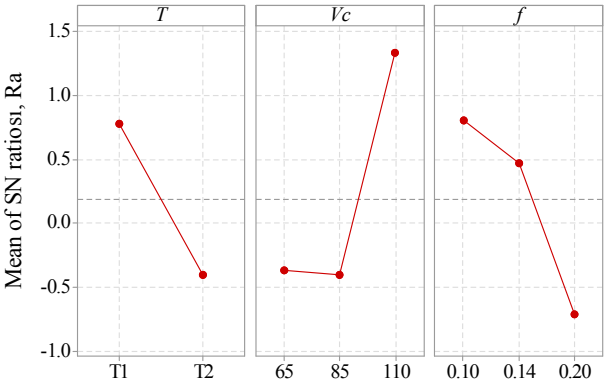

Figure 4. Main effects plot for S/N ratios of surface roughness.

For the CFRP/metallic stacks, the effect of the feed rate on the shape and size of the chip was more important than its effect on the initiation of chip formation in the CARALL composite or than the amount of deformation of the aluminum layer in the direction of the feed rate. Drilling at high feed rates caused the cutting tool to be exposed to a higher chip load per unit of time, and as the cutting tool did not have enough time for a proper drilling, the compacting pressure on the layers of the laminate increased. In this case, apart from the lack of an efficient drilling process, the cutting tool caused downward deformation of the AL5754 layers, and the *Ra* values increased with the increased fiber separation in the CFRP layers.

The ANOVA results for surface roughness depending on the control factors are presented in Table 5. The most effective and only significant (P<0.05) parameter among the control factors was observed to be the *T*Vc* interaction, with a 66.504% contribution ratio, followed by cutting speed, with a 9.55% contribution.

Table 5. ANOVA results for surface roughness

Control factors	DoF	SS	MS	F_table	P	Contribution %
T	1	6.239	6.2387	6.26	0.067	5.030
Vc	2	11.846	5.923	5.94	0.063	9.551
f	2	7.648	3.8239	3.83	0.118	6.166
*T*Vc*	2	82.483	41.2416	41.35	0.002*	66.504
*T*f*	2	3.724	1.862	1.87	0.268	3.003
*Vc*f*	4	8.098	2.0244	2.03	0.255	6.529
Residual Error (e)	4	3.989	0.9974			3.216
Total	17	124.027				100
R^2=96.8% Adjusted R^2=86.3%						
DoF: Degree of freedom, SS: Sum of squares, MS: Mean square *: Statistically significant effective parameter						

3.2.3. Delamination factor

Composite damage is known to cause a large decrease in mechanical performance because of crack propagation [41]. Delamination results when the axial thrust force acting on the layers exceeds the shear strength between the plates during drilling [42]. During the drilling of carbon/epoxy composites, damage occurs readily at the hole exit. Major damage includes delamination, flaking, and fiber pullout. Figure 5 presents the S/N ratio main effects plot for the delamination factor (*Df*) at the hole exit during the drilling of the CARALL composite. Lower *Df* values were obtained with the uncoated tool. Cutting temperature and cutting force are two important factors that determine the machining quality of carbon/epoxy composites. Figure 3 shows that the uncoated tool produced a lower thrust force compared to the signum-coated tool. The thrust force is considered to be a key factor in causing damage such as delamination, and greater thrust force leads to more damage [38]. Low cutting speeds caused higher temperature formation [39]. With increasing temperatures, matrix properties were weakened and fiber-epoxy interface strength as well as laminar strength decreased. This low interlaminar strength and low fiber-epoxy interface strength near the hole exit resulted in delamination, flaking, and fiber stripping [38]. Increasing cutting forces with increasing feed rate compounded the delamination damage. Many researchers have reported in the literature that increasing feed rate with the increase of the thrust forces caused delamination damage to increase [43-47]. Xu et al. stated that when drilling fiber reinforced composites, high cutting speed and low feed rates should be selected

in order to reduce the delamination damage at the hole exit [20].

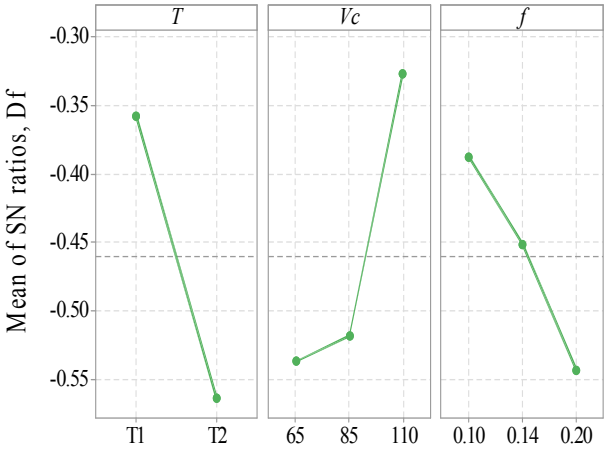

Figure 5. Main effects plot for S/N ratios of delamination factor.

The ANOVA results for *Df* depending on the control factors are presented in Table 6. In terms of control factor and factor interactions, the tool coating condition and cutting speed were seen to have a significant ($P < 0.05$) effect on *Df*. The most effective control factor in terms of impact on the *Df* was the tool coating condition, with a 29.13% contribution ratio, followed by the cutting speed and the interaction of *Vc*f* with 24.61% and 21.52% contribution ratios, respectively.

Table 6. ANOVA results for delamination factor

Control factors	DoF	SS	MS	F_table	P	Contribution %
T	1	0.19129	0.191292	18.19	0.013*	29.137
Vc	2	0.16159	0.080793	7.68	0.043*	24.613
f	2	0.07316	0.036581	3.48	0.133	11.143
*T*Vc*	2	0.01824	0.009119	0.87	0.487	2.778
*T*f*	2	0.02885	0.014425	1.37	0.352	4.394
*Vc*f*	4	0.14132	0.035331	3.36	0.134	21.525
Residual Error (e)	4	0.04208	0.010519			6.409
Total	17	0.65653				100.000

R^2=93.6%, Adjusted R^2=72.8%, DoF: Degree of freedom,
SS: Sum of squares, MS: Mean square,
*: Statistically significant effective parameter

3.3 Multi-Objective Optimization of Process Parameters with Taguchi-Based GRA-PCA

In order to reach the optimum levels of a series of control factors that provide the lowest *Ft*, *Ra,* and *Df* values, the Taguchi-based GRA-PCA optimization technique was applied, respectively. In our study, the response variables could not be compared because they used different units. For this reason, first, the experimental results (*Ft*, *Ra,* and *Df* values) were normalized according to "the smaller is better" criterion via Equation (2) and transformed into dimensionless numbers, as presented in Table 7.

The GRC estimates for each experiment were calculated via Equations (3)-(6) and are presented in Table 10. The weight ratios used in the GRD calculation were determined via PCA. Table 8 shows that the variance participation from the first eigenvalue of the principal component (PC) is characterized at a high level (57.61%). For this reason, the square of the eigenvector of PC1 presented in Table 9 was used to determine the weights of the quality characteristics.

Table 7. Experimental data and normalized values.

No	Control factors			Experimental data			Normalized values		
	T	*Vc* [m/min]	*f* [mm/rev]	*Ft* [N]	*Ra* [μm]	*Df*	*Ft*	*Ra*	*Df*
1	Uncoated tool	65	0.1	179.040	1.074	1.015	0.8214	0.5454	1.0000
2		65	0.14	208.337	1.223	1.057	0.5000	0.4125	0.5866
3		65	0.2	240.883	1.686	1.067	0.1429	0.0000	0.4826
4		85	0.1	169.273	1.178	1.063	0.9286	0.4532	0.5250
5		85	0.14	221.350	0.950	1.048	0.3572	0.6563	0.6716
6		85	0.2	238.227	0.898	1.048	0.1720	0.7022	0.6696
7		110	0.1	162.763	0.586	1.020	1.0000	0.9802	0.9505
8		110	0.14	195.313	0.611	1.036	0.6429	0.9577	0.7889
9		110	0.2	234.373	0.564	1.024	0.2143	1.0000	0.9117
10	Signum-coated tool	65	0.1	179.037	0.702	1.069	0.8215	0.8771	0.4656
11		65	0.14	218.097	0.821	1.060	0.3929	0.7710	0.5511
12		65	0.2	244.140	1.013	1.116	0.1072	0.6000	0.0000
13		85	0.1	169.273	1.027	1.069	0.9286	0.5873	0.4668
14		85	0.14	218.097	1.054	1.056	0.3929	0.5630	0.5937
15		85	0.2	240.883	1.220	1.084	0.1429	0.4156	0.3162
16		110	0.1	179.037	1.078	1.039	0.8215	0.5419	0.7631
17		110	0.14	211.587	1.176	1.062	0.4643	0.4543	0.5353
18		110	0.2	253.907	1.558	1.049	0.0000	0.1147	0.6615

Table 8. Eigenvalues and contribution percentages for the principal components

Principal components	Eigenvalues	Percentage of contribution (%)
First (PC1)	1.7282	57.61
Second (PC2)	0.6576	21.92
Third (PC3)	0.6142	20.47

In Equation (10), the GRD values were calculated using the weights determined in Table 9 (0.35, 0.33, and 0.32 for y_{m1}, y_{m2} and y_{m3} values, respectively) and these values are presented in Table 10.

Table 9. Eigenvectors and weights for principal components

Control factors	Eigenvectors			Weights
	PC1	PC2	PC3	
Ft	0.588	-0.16	-0.793	0.35
Ra	0.576	-0.0605	0.549	0.33
Df	0.568	0.78	0.263	0.32

A GRD value of 1 or close to 1 represents optimal drilling conditions. As seen in Table 10, ideal machining conditions, i.e., the highest GRD value (0.5530), were reached in experiment no. 7 (110 m/min cutting speed, 0.1 mm/rev feed rate, and uncoated tool).

The experiments were ranked in terms of GRD values as: experiments no. 7 (1st), 1 (2nd), and 9 (3rd).

Table 10. Gray relational response variables

No	Normalization			GRC			GRD	Rank
	T	*Vc* [m/min]	*f* [mm/rev]	*Ft*	*Ra*	*Df*		
1	Uncoated tool	65	0.1	0.7368	0.5238	1.0000	0.4343	2
2		65	0.14	0.5000	0.4598	0.5474	0.2899	13
3		65	0.2	0.3684	0.3333	0.4914	0.2293	18
4		85	0.1	0.8750	0.4777	0.5128	0.3603	8
5		85	0.14	0.4375	0.5927	0.6036	0.3138	10
6		85	0.2	0.3765	0.6267	0.6021	0.3081	11
7		110	0.1	1.0000	0.9619	0.9099	0.5530	1
8		110	0.14	0.5833	0.9220	0.7032	0.4245	4
9		110	0.2	0.3889	1.0000	0.8499	0.4291	3
10	Signum-coated tool	65	0.1	0.7369	0.8026	0.4834	0.3901	5
11		65	0.14	0.4516	0.6859	0.5269	0.3200	9
12		65	0.2	0.3590	0.5556	0.3333	0.2401	17
13		85	0.1	0.8750	0.5478	0.4839	0.3683	7
14		85	0.14	0.4516	0.5336	0.5517	0.2954	12
15		85	0.2	0.3684	0.4611	0.4224	0.2407	16
16		110	0.1	0.7369	0.5219	0.6786	0.3731	6
17		110	0.14	0.4828	0.4782	0.5183	0.2846	14
18		110	0.2	0.3333	0.3609	0.5963	0.2475	15

The main effects plot for the GRD is presented in Figure 6. For ideal response variables, a GRD value close to 1 is desirable. Table 10 indicates that the highest GRD values were reached with the uncoated tool at 110 m/min cutting speed and 0.1 mm/rev feed rate (experiment no. 7). It was determined that the uncoated tool, high cutting speed, and low feed rate had a positive effect on the response variables.

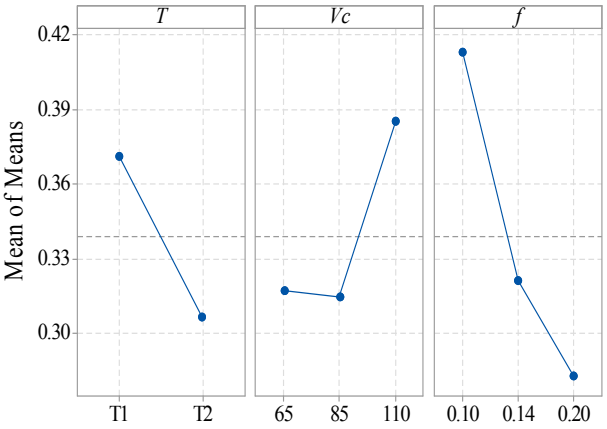

Figure 6. Main effects plot for gray relational degree.

The ANOVA results for the GRD are presented in Table 11. The most effective control factor for all three responses was found to be the feed rate, with a contribution ratio of 47.2%, followed by tool coating condition-cutting speed interaction (17.19%), tool coating condition (13.9%), and cutting speed (13.11%).

Table 11. ANOVA results for GRD

Control factors	DoF	SS	MS	F_table	P	Contribution %
T	1	10.615	10.6148	22.46	0.009*	13.90
Vc	2	10.007	5.0035	10.59	0.025*	13.11
f	2	36.113	18.0563	38.21	0.002*	47.29
*T*Vc*	2	13.126	6.5631	13.89	0.016*	17.19
*T*f*	2	1.002	0.5012	1.06	0.427	1.31
*Vc*f*	4	3.607	0.9016	1.91	0.273	4.72
Residual Error (e)	4	1.89	0.4726			2.48
Total	17	76.36				100
R^2=97.5%, Adjusted R^2=89.5%, DoF: Degree of freedom, SS: Sum of squares, MS: Mean square *: Statistically significant effective parameter						

4. CONCLUSION

The following results were obtained in terms of the cutting forces, surface roughness, and delamination factor in the drilling of the CARALL composite, depending on the cutting parameters and tool coating condition.

- Probability tests were performed on the *Ft*, *Ra,* and *Df* results obtained depending on the control factor levels. As a result of these tests, P values were calculated as 0.13, 0.434, and 0.414, respectively, and it was found that the AD values for *Ft*, *Ra,* and *Df* (0.554, 0.349, and 0.358, respectively) were lower than the critical value of 0.752 and therefore, they were suitable for optimization.
- The thrust force values varied between 162.763 and 253.907 N and increased significantly with the feed rate; however, they decreased with increasing cutting speed. The ANOVA results showed that the feed rate was the most effective drilling parameter, with a 93.87% contribution ratio. No significant effect (<2%) was found for tool coating or cutting speed.
- Surface roughness values varied between 0.564 and 1.686 μm. The most effective parameter on surface roughness was the tool coating status-cutting speed interaction, with a 66.504% contribution ratio.
- Delamination factor values varied in the range of 1.015-1.084 and the most effective control factor according to the ANOVA results was the tool coating condition, with a 29.13% contribution ratio, followed by cutting speed (24.61%), and cutting speed-feed rate interaction (21.52%).
- As a result of the hybrid GRA-PCA multi-objective optimization, the optimum machining conditions to achieve minimum *Ft*, *Ra,* and *Df* when drilling the CARALL composite with uncoated and coated carbide tools were determined as 110 m/min cutting speed, 0.1 mm/rev feed rate, and the uncoated cutting tool, respectively.

- The ANOVA results for GRD indicated that the most effective control factor was the feed rate, with a 47.29% contribution ratio, followed by the interaction of tool coating condition-cutting speed, tool coating condition, and cutting speed, respectively.

As a continuation of this study, our future research will investigate the delamination factor and hole quality in the drilling of CARALL using drills of different tool geometries. Our future research is important in terms of evaluating the effects of tool geometry as well as those of coating properties. Finally, we will also examine the effects of fiber orientation on hole quality and delamination damage in FMLs.

ACKNOWLEDGMENT

The authors would like to express their sincere thanks to the Çanakkale Onsekiz Mart University Scientific Research Projects Unit for support of the project (No. FBA-2019-3170)

REFERENCES

[1] Zweben CH, Beaumont P.W.R., editors. Comprehensive Composite Materials II. 2nd Edition. Elsevier; 2018

[2] Jawaid M, Thariq M, editors. Sustainable Composites for Aerospace Applications. 1st Edition. Woodhead Publishing; 2018.

[3] Seo, H.: Damage tolerance and durability of GLARE laminates, ProQuest, 2008.

[4] Krishnakumar, S.: Fibre metal laminates–the synthesis of metal and composite. Mater. Manuf. Process., Vol. 9, No: 2, pp. 295–354, 1994.

[5] Purnowidodo, A., Iman, H.,: Crack propagation behavior on metal laminate of FMLs after a high tensile overload under high constant amplitude load., FME Transactions, Vol. 48, No. 2, pp. 419–426, 2020.

[6] Sinmazçelik, T., Avcu. E., Bora. M.Ö. and Çoban, O.: A review: Fibre metal laminates, background, bonding types and applied test methods, Mater. Des., Vol. 32, pp. 3671–3685, 2011.

[7] Mangalgiri, P.D.: Composite material for aerospace applications, Bull. Mater. Sci., Vol. 22, No. 3, pp. 656-664,1999.

[8] Mouritz, A.: Introduction to aerospace materials. Elsevier, 2012.

[9] Beaumont P.W.R., Soutis C. and Hodzic A. (Editors): Structural integrity and durability of advanced composites: Innovative modelling methods and intelligent design, Woodhead Publishing - Elsevier, Cambridge, UK, 2015.

[10] Xu, J., Li, C., Chen, M., El Mansori, M. and Ren, F.: An investigation of drilling high-strength CFRP composites using specialized drills, Int. J. Adv. Manuf. Technol., Vol. 103, pp. 3425–3442, 2019.

[11] Pawar, O.A., Gaikhe, Y.S., Tewari, A., Sundaram, R. and Joshi, S.S. Analysis of hole quality in drilling GLARE fiber metal laminates, Compos. Struct., Vol. 123, pp. 350–365, 2015.

[12] Tyczynski, P., Lemanczyk, J. and Ostrowski, R.: Drilling of CFRP, GFRP, GLARE type composites, Aircr. Eng. Aerosp. Tec., Vol. 86, No. 4, pp. 312–322, 2014.

[13] Coesel, J.F.W.: Drilling of fibre-metal laminates, Master Thesis. Delft University of Technology, Delft, 1994.

[14] Giasin, K., Gorey, G., Byrne, C., Sinke, J. and Brousseau, E.: Effect of machining parameters and cutting tool coating on hole quality in dry drilling of fibre metal laminates, Compos. Struct., Vol. 212, pp. 159–174, 2019.

[15] Giasin, K., Ayvar-Soberanis, S., French, T. and Phadnis, V.: 3D finite element modelling of cutting forces in drilling fibre metal laminates and experimental hole quality analysis, Appl. Compos. Mater., Vol. 24, pp. 113–137, 2017.

[16] Giasin, K., Ayvar-Soberanis, S. and Hodzic, A.: An experimental study on drilling of unidirectional GLARE fibre metal laminates, Compos. Struct., Vol.133, pp. 794–808. 2015.

[17] Sorrentino, L,, Turchetta, S. and Bellini, C.: A new method to reduce delaminations during drilling of FRP laminates by feed rate control, Compos. Struct., Vol. 186, pp. 154–64, 2018.

[18] Silva, D., Pamies Teixeira, J. and Machado, C.M.: Methodology analysis for evaluation of drilling induced damage in composites, Int. J. Adv. Manuf. Technol., Vol. 71, No. 9, pp. 1919–1928. 2014.

[19] Samuel Raj, D. and Karunamoorthy, L.: Cutting edge-flatting and roughness measurement to monitor blunting and chipping of the drill cutting edge when drilling CFRP, Int. J. Adv. Manuf. Technol., Vol. 92, No. 1, pp. 953–68, 2017.

[20] Xu, J., Li, C., Mi, S., An, Q. and Chen, M.: Study of drilling-induced defects for CFRP composites using new criteria. Compos. Struct. Vol. 201, pp. 1076–1087, 2018.

[21] Caggiano, A., Angelone, R. and Teti, R.: Image analysis for CFRP drilled hole quality assessment. Procedia CIRP., Vol. 62, pp. 440–445, 2017.

[22] Lissek, F, Tegas, J. and Kaufeld, M.: Damage quantification for the machining of CFRP: An introduction about characteristic values considering shape and orientation of drilling-induced delamination. Proc. Eng. Vol. 149, pp. 2–16, 2016.

[23] Davim, J.P. and Reis, P.: Study of delamination in drilling carbon fiber reinforced plastics (CFRP) using design experiments, Compos. Struct., Vol. 59, pp. 481–487, 2003.

[24] Ranjit, K. R.: Design of experiments using the Taguchi Approach: 16 Steps to Product and Process Improvement, John Wiley & Sons, USA, 2001.

[25] Gohil, V. and Puri, Y.M.: Optimization of electrical discharge turning process using Taguchi-grey relational approach, Procedia CIRP, Vol.68, pp.70–75, 2018.

[26] Chinnaiyan, P. and Jeevanantham, A.K.: Multi-objective optimization of single point incremental

sheet forming of AA5052 using Taguchi based grey relational analysis coupled with principal component analysis, Int. J. Precis. Eng. Manuf., Vol. 15, pp. 2309–2316, 2014.

[27] Razak, M.A., Abdul-Rani, A.M., Rao, T.V.V.L.N., Pedapati, S.R. and Kamal, S.: Electrical discharge machining on biodegradable AZ31 magnesium alloy using Taguchi method. Proc. Eng., Vol. 148, pp. 916–922, 2016.

[28] Yan, J. and Li, L.: Multi-objective optimization of milling parameters–the trade-offs between energy, production rate and cutting quality, J. Clean. Prod., Vol.52, pp. 462-471, 2013.

[29] Xu, J. and El Mansori, M.: Experimental study on drilling mechanisms and strategies of hybrid CFRP/Ti stacks, Compos. Struct, Vol. 157, pp. 461–482, 2016.

[30] Montoya, M., Calamaz, M., Gehin, D. and Girot, F.: Evaluation of the performance of coated and uncoated carbide tools in drilling thick CFRP/aluminum alloy stacks., Int. J Adv. Manuf. Technol., Vol. 68, No. 9, pp. 2111–2120, 2013.

[31] Alizadeh Ashrafi, S., Sharif, S., Akhavan Farid, A. and Yahya, M.Y.: Performance evaluation of carbide tools in drilling CFRP-Al stacks. J. Compos. Mater., Vol. 48, No. 17, pp. 2071–2084, 2014.

[32] Eneyew, E.D. and Ramulu, M.: Experimental study of surface quality and damage when drilling unidirectional CFRP composites, J. Mater. Res. Technol., Vol. 3, No. 4, pp. 354–62, 2014.

[33] Karpat, Y. and Bahtiyar, O.: Tool geometry based prediction of critical thrust force while drilling carbon fiber reinforced polymers. Int. J. Adv. Manuf. Technol., Vol. 3, No. 4, pp. 300–308, 2015.

[34] Wang, C-Y., Chen, Y-H., An, Q-L., Cai, X-J., Ming, W-W. and Chen, M.: Drilling temperature and hole quality in drilling of CFRP/aluminum stacks using diamond coated drill, Int. J. Precis. Eng. Manuf., Vol. 6, No. 8, pp. 1689–1697, 2015.

[35] Park, S.Y., Choi, W.J., Choi, C.H. and Choi, H.S.: Effect of drilling parameters on hole quality and delamination of hybrid GLARE laminate, Compos. Struct, Vol. 185, pp. 684–698, 2018.

[36] Kumar, J., Verma, R.V.: Experimental investigations and multiple criteria optimization during milling of graphene oxide (GO) doped epoxy/CFRP composites using TOPSIS-AHP hybrid module., FME Transactions, Vol. 48, No. 3, pp. 628–635, 2020.

[37] Giasin, K.: Machining Fibre Metal Laminates and Al2024-T3 aluminium alloy. University of Sheffield; 2017.

[38] Wang, B., Gao, H., Cao, B., Zhuang, Y. and Zhao, Z.: Mechanism of damage generation during drilling of carbon/epoxy composites and titanium alloy stacks, Proc IMechE Part B: J Engineering Manufacture, Vol. 228, No. 7, pp. 698–706, 2014.

[39] Merino-Pérez, J.L., Royer, R. Ayvar-Soberanis, S., Merson, E. and Hodzic, A.: On the temperatures developed in CFRP drilling using uncoated WC-Co tools Part I: Workpiece constituents, cutting speed and heat dissipation, Compos. Struct, Vol. 123, pp. 161–168, 2015.

[40] Zitoune, R., Krishnaraj, V., Collombet, F. and Le Roux, S.: Experimental and numerical analysis on drilling of carbon fibre reinforced plastic and aluminum stacks, Compos. Struct., Vol. 146, pp.148–158, 2016.

[41] Romoli, L. and Lutey, A.H.A.: Quality monitoring and control for drilling of CFRP laminates, J. Manuf. Process, Vol. 40, pp. 16–26, 2019.

[42] Kakkassery, J.J., Arumugam, V., Saravanakumar, K., Durga, S., Santulli, C., Pavlovic, A.: Residual strength estimation and damage characterization by acoustic emission of drilled thermally conditioned fiberglass laminates., FME Transactions, Vol. 46, No. 4, pp. 489–496, 2018.

[43] Grilo, T.J., Paulo, R.M.F., Silva, C.R.M., Davim, J.P.: Experimental delamination analyses of CFRPs using different drill geometries. Compos. Part. B Eng. Vol. 45, No. 1, pp. 1344–1350, 2013.

[44] Krishnaraj, V., Prabukarthi, A., Ramanathan, A., Elanghovan, N., Senthil Kumar, M., Zitoune, R., et al: Optimization of machining parameters at high speed drilling of carbon fiber reinforced plastic (CFRP) laminates, Compos. Part. B Eng., Vol. 43, No. 4, pp. 1791–1799, 2012.

[45] Melentiev, R., Priarone, P.C., Robiglio, M. and Settineri, L.: Effects of tool geometry and process parameters on delamination in CFRP drilling: An overview., Proc. CIRP, Vol. 45, pp. 31–44, 2016.

[46] Feito, N., Diaz-Álvarez, J., López-Puente, J. and Miguelez, M.H.: Numerical analysis of the influence of tool wear and special cutting geometry when drilling woven CFRPs, Compos. Struct., Vol. 138, pp. 285–94, 2016.

[47] Gaitonde, V.N., Karnik, S.R., Rubio, J.C., Correia, A.E., Abrão, A.M. and Davim, J.P.: Analysis of parametric influence on delamination in high-speed drilling of carbon fiber reinforced plastic composites., J. Mater. Process. Technol., Vol. 203, No. 1, pp. 431–438, 2008.

ВИШЕЦИЉНА ОПТИМИЗАЦИЈА ПАРАМЕТАРА ПРОЦЕСА БУШЕЊА МЕТАЛНОГ ЛАМИНАТА ОЈАЧАНОГ ВЛАКНИМА КОРИШЋЕЊЕМ ХИБРИДНОГ GRA-PCA ПРИСТУПА

Е. Екици, А.Р. Моторџу, Г. Узун

Истражује се утицај параметара бушења и стања превлаке резног алата на потисну силу, површинску храпавост и фактор деламинације код CARALL композитног материјала, врсту комерцијалног металног ламината ојачаног влакнима. Грејрелациона анализа (GRA) је коришћена као метод вишецињне оптимизације за одређивање оптималних параметара обраде, док су анализом главних компонената (PCA) од-

рађени тежински коефицијенти. Према резултатима експеримента најзначајнији контролни фактори код потисне силе, површинске храпавости и фактора деламинације су брзина помоћног кретања, интеракција између превлаке алата и брзине резања, стање превлаке резног алата: 93,87% односно 66,504% односно 29,137%. На основу резултата GRA-PCA анализе одређен је оптимални ниво контролних фактора: брзина резања - 110 м/мин, брзина помоћног кретања – 0,1 мм/мин и алат без превлаке.